

Complexity Generation in Fungal Peptidyl Alkaloid Biosynthesis: A Two-Enzyme Pathway to the Hexacyclic MDR Export Pump Inhibitor Ardeemin

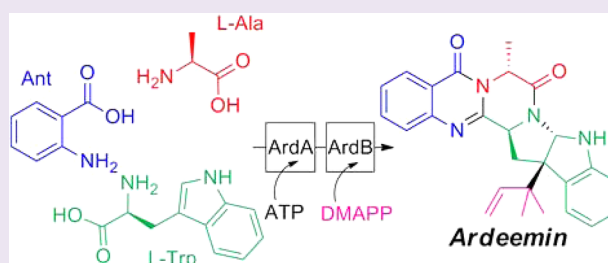
Stuart W. Haynes,[†] Xue Gao,[‡] Yi Tang,^{*,‡,§} and Christopher T. Walsh^{*,†}

[†]Department of Biological Chemistry and Molecular Pharmacology, Harvard Medical School, 240 Longwood Avenue, Boston, Massachusetts 02115, United States

[‡]Department of Chemical and Biomolecular Engineering and [§]Department of Chemistry and Biochemistry, University of California Los Angeles, 420 Westwood Plaza, Los Angeles, California 90095, United States

Supporting Information

ABSTRACT: Ardeemins are hexacyclic peptidyl alkaloids isolated from *Aspergillus fischeri* as agents that block efflux of anticancer drugs by MultiDrug Resistance (MDR) export pumps. To evaluate the biosynthetic logic and enzymatic machinery for ardeemin framework assembly, we sequenced the *A. fischeri* genome and identified the *ardABC* gene cluster. Through both genetic deletions and biochemical characterizations of purified ArdA and ArdB we show this ArdAB enzyme pair is sufficient to convert anthranilate (Ant), L-Ala, and L-Trp to ardeemin. ArdA is a 430 kDa trimodular nonribosomal peptide synthase (NRPS) that converts the three building blocks into a fumiquinazoline (FQ) regioisomer termed ardeemin FQ. ArdB is a prenyltransferase that takes tricyclic ardeemin FQ and dimethylallyl diphosphate to the hexacyclic ardeemin scaffold via prenylation at C₂ of the Trp-derived indole moiety with intramolecular capture by an amide NH of the fumiquinazoline ring. The two-enzyme ArdAB pathway reveals remarkable efficiency in construction of the hexacyclic peptidyl alkaloid scaffold.



Members of the fungal genus *Aspergillus* make a variety of peptidyl alkaloids based around the nonproteinogenic aryl β -amino acid anthranilate (Ant).^{1–4} They show a wide range of biological activities, including tremorgens such as tryptoquialanines,⁵ developmentally regulated fumiquinazolines,⁶ asperlicins that act as cholecystokinin antagonists,^{7,8} and ardeemins that block MDR export pumps in tumor cells.^{9,10} The fungi build these complex multicyclic quinazolinone scaffolds from two to four amino acids in short efficient pathways.

The peptidyl alkaloid frameworks arise from amino acid building blocks selected and elongated by nonribosomal peptide synthetase (NRPS) machinery,¹¹ which are then further processed by dedicated post assembly line tailoring enzymes for oxidations, acylations, and alkylations (e.g., prenylations). The nonproteinogenic aryl β -amino acid anthranilate along with the proteinogenic tryptophan are key constituents of the multicyclic scaffolds of aszonalenins,¹² fumiquinazolines,¹³ and the tryptoquialanines.⁵

We have recently deciphered the fungal code for anthranilate-activating NRPS adenylation domains in *Aspergillus* species and demonstrated that anthranilate is the chain-initiating unit.¹³ In bimodular NRPS enzymes, Ant activation is followed by L-Trp to generate aszonalenin,¹² or in a trimodular NRPS system,^{13,14} the ~450 kDa proteins follow Ant with both Trp and L-Ala and convert the three building blocks into the tricyclic (6,6,6) fumiquinazoline F scaffold

(Scheme 1). We have shown this scaffold to be a common early intermediate in both the generation of the heptacyclic fumiquinazoline C in *Aspergillus fumigatus*^{6,15,16} and the production of the neurotoxic tryptoquialanines⁵ by *Penicillium aethiopicum*.¹⁴

The hexacyclic ardeemins (Figure 1) were isolated from *Aspergillus fischeri* on the basis of their ability to reverse multidrug resistance phenotypes both in isolated cells and in mammary carcinoma xenografts^{9,10} by binding to P-glycoprotein export pumps.^{17,18} The ardeemin name comes from this property: the ability to reverse drug insensitivity. Ardeemins were shown to result in sensitization to vinca antitumor alkaloids by up to 700 fold.¹⁹ Danishefsky and colleagues have led synthetic efforts toward the ardeemins and termed them “reverse prenyl hexahydropyrrolo[2,3-*b*]indole alkaloids”.²⁰

Inspection of the ardeemin scaffold indicates a tripeptide origin, with the same three building blocks as the fumiquinazoline system, anthranilate, alanine, and tryptophan, but the connectivity and the tailoring enzyme operations must be distinct from the fumiquinazoline system. After construction of the core structure, a subsequent intramolecular, complexity-building cyclization should be mediated in ardeemin by

Received: December 10, 2012

Accepted: January 20, 2013

Published: January 20, 2013

Scheme 1. Differentiation in NRPS Mediated Biosynthesis of FQF and Ardeemin FQ: Formation of Regioisomeric Quinazolinones by Swapping the Order of A Domains

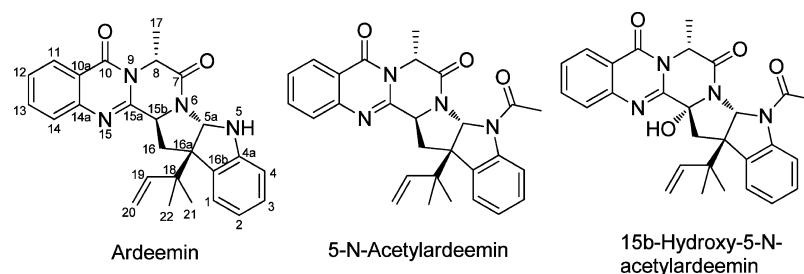
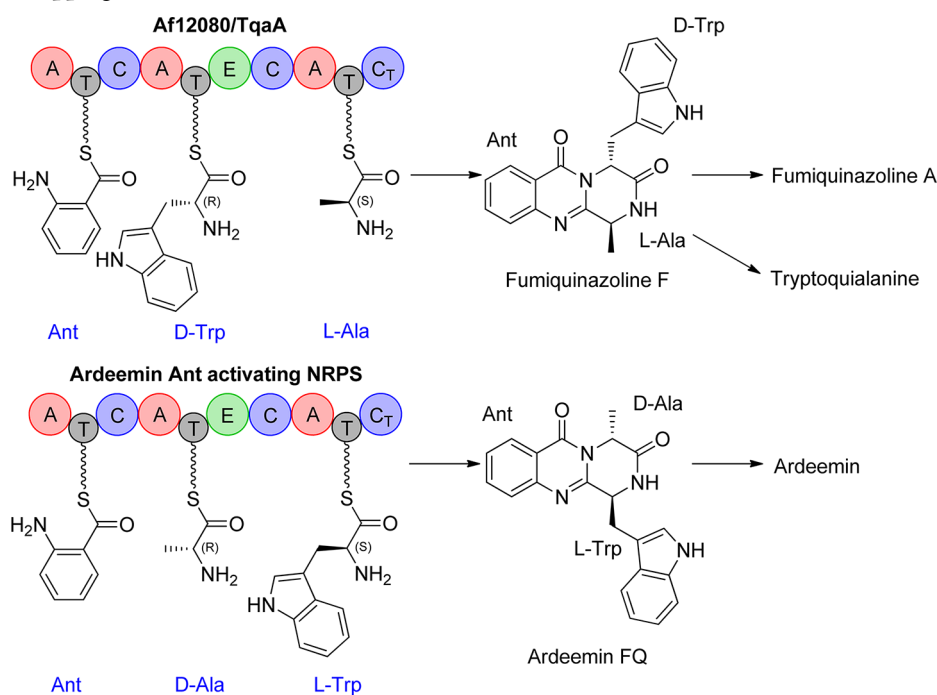


Figure 1. Structures of ardeemins.

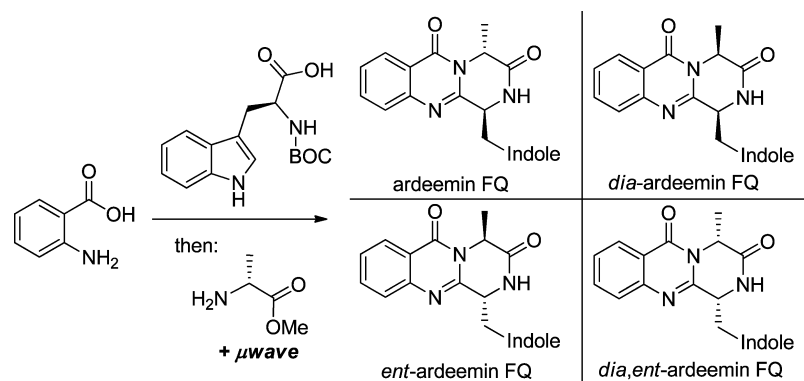


Figure 2. Synthetic route to ardeemin FQ and illustration of isomers observed.

prenylation with reverse regiochemistry at the β -carbon of the pyrrole ring of a Trp moiety. The immediate precursor in such a ring-closing prenylation should be a 6,6,6-tricyclic pyrazinoquinazolinone, related to but distinct from fumiquinazoline F (termed here ardeemin fumiquinazoline = ardeemin FQ) by different placement of the Ala- and Trp-derived side chains on the same tricyclic scaffold. The distinction could arise from the putative ardeemin-forming NRPS acting in the order Ant-Ala-

Trp rather than the order Ant-Trp-Ala seen in the fumiquinazoline and tryptoquialanine pathways (Scheme 1 and Figure 1).^{5,13,14}

In this study we have validated these predictions by the identification of the ardeemin biosynthetic gene cluster in *A. fischeri*, detection of the ardeemin tricyclic intermediate from a trimodular NRPS enzyme, and generation of hexacyclic

ardeemin by the action of a single prenyltransferase on the tricyclic ardeemin FQ intermediate.

RESULTS AND DISCUSSION

Synthesis of Tricyclic Ardeemin Fumiquinazoline (Ardeemin FQ) Diastereomers As Metabolite Standards.

As prelude to biological evaluation of the ardeemin biosynthetic pathway, in accord with the proposal in Scheme 1 that ardeemin would arise from prenylation-induced cyclization of the tricyclic precursor ardeemin FQ, we undertook its synthesis from anthranilate and D-alanine and L-tryptophan by microwave accelerated condensation by analogy with the published procedure for the synthesis of FQF (as described in Supporting Information).²¹ Despite using enantiopure amino acids during this reaction, we observed pairs of diastereomers in the reaction mixture as a result of the epimerization of the two asymmetric centers. Fortunately these diastereomers proved to be readily separable by reverse phase HPLC into pairs of enantiomers, ardeemin FQ/*ent*-ardeemin FQ and *dia*-ardeemin FQ/*dia,ent*-ardeemin FQ (Figure 2). NMR spectroscopic analysis allowed both diastereomers to be fully characterized (see Supporting Information). Further preparative HPLC purification, this time over a homochiral stationary phase, allowed separation of the individual enantiomers. The preparation of synthetic ardeemin FQ (and diastereomers) proved to be mutually beneficial to the metabolite analysis of wild-type *A. fischeri* (discussed in later sections). The availability of synthetic ardeemin FQ allowed identification of the proposed biosynthetic intermediate during metabolite analysis. In turn the biosynthetic ardeemin FQ metabolite allowed us to identify the natural diastereomer and in turn match a synthetic enantiomer to natural ardeemin FQ (Supplementary Figures S4 and S5).

Bioinformatic Prediction of Ardeemin Biosynthetic Gene Cluster. Genome sequencing of *A. fischeri* var. *brasiliensis* (ATCC 96284) by Illumina sequencing generated 20.3 Gb of sequence giving approximately 677x coverage (assuming a 30 Mb genome) (statistics in Supplementary Table S1) and allowed mining of the assembled contigs for candidate biosynthetic gene clusters. We anticipated the ardeemin cluster (*ard*) should contain one gene encoding a trimodular NRPS, whose first adenylation domain should be specific for activation of anthranilate.¹³ We also anticipated there might be an associated prenyltransferase. One candidate cluster in *A. fischeri* fulfills these criteria. As shown in Figure 3a there is a predicted trimodular NRPS with the domains A-T-C-A-T-E-C-A-T-C_T that we have termed ArdA (A = adenylation, C = condensation, T = thiolation, E = epimerization domain, and C_T is a terminal cyclization domain^{14,22}). Based on the amino acid recognition code we have previously deciphered¹³ for the anthranilate-activating NRPS initiation modules for aszonalenein, for fumiquinazoline F, and for tryptoquialanine,^{5,13} the first module of ArdA will activate anthranilate. Module 2 (C-A-T-E) has a predicted epimerization domain, just what is required for the incorporation of D-Ala into the ardeemin backbone. Module 3 would then activate and incorporate L-Trp.

Immediately upstream of the *ardA* gene is an ORF we have labeled *ardB*, encoding a predicted dimethylallyl diphosphate-utilizing enzyme, a presumed prenyltransferase. Also, just upstream of this ORF is a predicted acetyltransferase, encoded by *ardC*, in line with the observations of *N*-acetylardeemin as part of the suite of *A. fischeri* natural products (Figure 1).¹⁰ A comparable pair of prenyltransferase (AnaPT, 31% identity/49% similarity to ArdB, Supplementary Figure S1) and

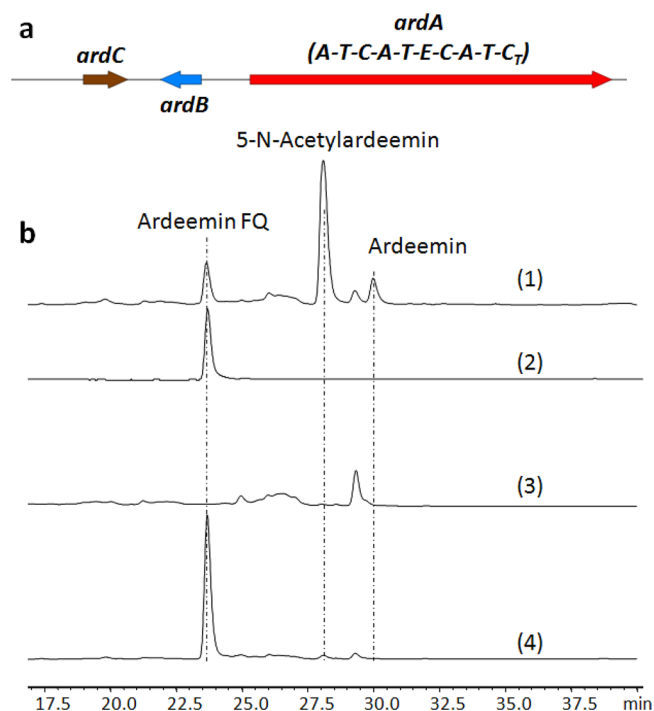


Figure 3. Identification of the ardeemin (*ard*) gene cluster. (a) Organization of the *ard* cluster. (b) HPLC analysis ($\lambda = 292$ nm) of 3-day metabolites produced by *A. fischeri* strains (1) WT *A. fischeri*; (2) synthetic ardeemin FQ standard; (3) *A. fischeri* with *ardA* KO; (4) *A. fischeri* with *ardB* KO.

acetyltransferase (AnaAT, 35% identity/53% similarity to ArdC, Supplementary Figure S2) enzymes accompanies the bimodular NRPS in the acetylazonalenein biosynthetic gene cluster.¹² Notably however, the examination of this cluster provides no explanation of origin of the other member of the ardeemin suite of natural products, 15b-hydroxy-5-*n*-acetyl ardeemin. There is no candidate enzyme present in or adjacent to this cluster to account for the incorporation of the hydroxyl group (Supplementary Table S4).

Genetic Deletion of *ardA* and *ardB* Validates Their Roles in Ardeemin Biosynthesis.

Genetic validation of *ardABC* as the ardeemin biosynthetic gene cluster was achieved by gene deletions and examination of the effect on secreted metabolites. As shown in Figure 3b trace 1, extracted metabolites from the parent *A. fischeri* culture yield UV-detectable peaks with the masses of 5-*N*-acetylardeemin (calculated = 469.2234; observed = 469.2232), ardeemin (calculated = 427.2129; observed = 427.2130), and also of the predicted ardeemin FQ (calculated = 359.1503; observed = 359.1506). This novel metabolite, predicted to be ardeemin FQ, co-chromatographed with synthetic ardeemin FQ (as noted above) and was distinct from the mobility of *dia*-ardeemin FQ (from microwave synthesis) (Figure 3b and Supplementary Figure S4).

Disruption of the *ardA* gene by insertion of the *bar* marker, which confers resistance to glufosinate,²³ (validated by PCR analysis, Supplementary Figure S3) resulted in loss of both metabolites (Figure 3b trace 3 and Supplementary Figure S4). Thus, the NRPS enzyme ArdA operates at the earliest stage of ardeemin assembly. A similar insertion into the *ardB* gene resulted in loss of mature ardeemin but accumulation of ardeemin FQ (Figure 3b trace 4 and Supplementary Figure S4), in accord with our assignment of ArdB as a prenyltransferase

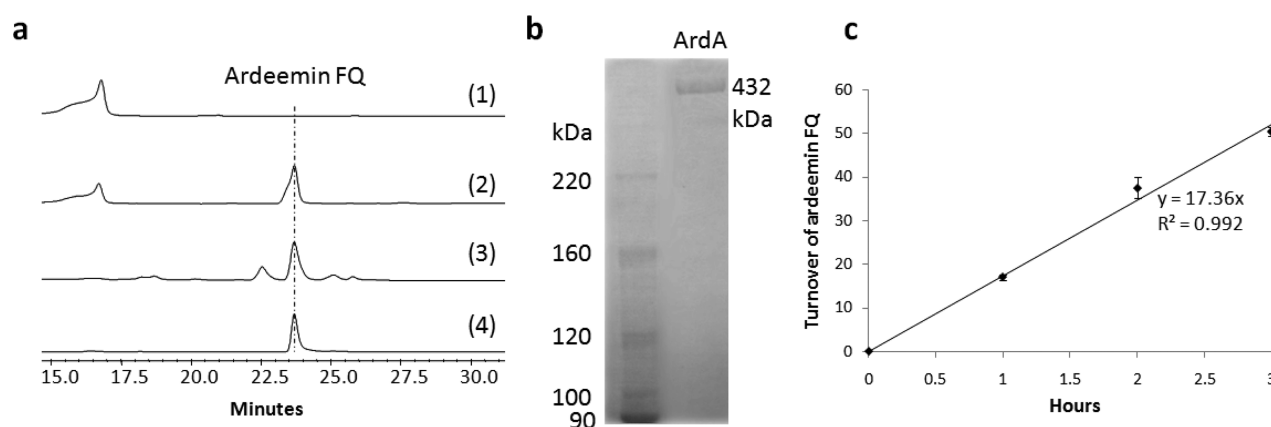


Figure 4. Characterization of ArdA. (a) HPLC analyses (at $\lambda = 292$ nm) of *in vivo* and *in vitro* reconstitution of ArdA. (1) 2 mM amino acid building blocks and no enzyme, (2) 2 mM amino acid building blocks and 10 μ M ArdA, (3) metabolites extracted from 3-day culture of BJS464-NpgA expressing ArdA, (4) synthetic ArdFQ synthetic standard. (b) SDS-PAGE of the heterologously expressed ArdA protein purified by FLAG-tag affinity chromatography (432 kDa). (c) HPLC-based time course study of the turnover of ArdFQ by ArdA.

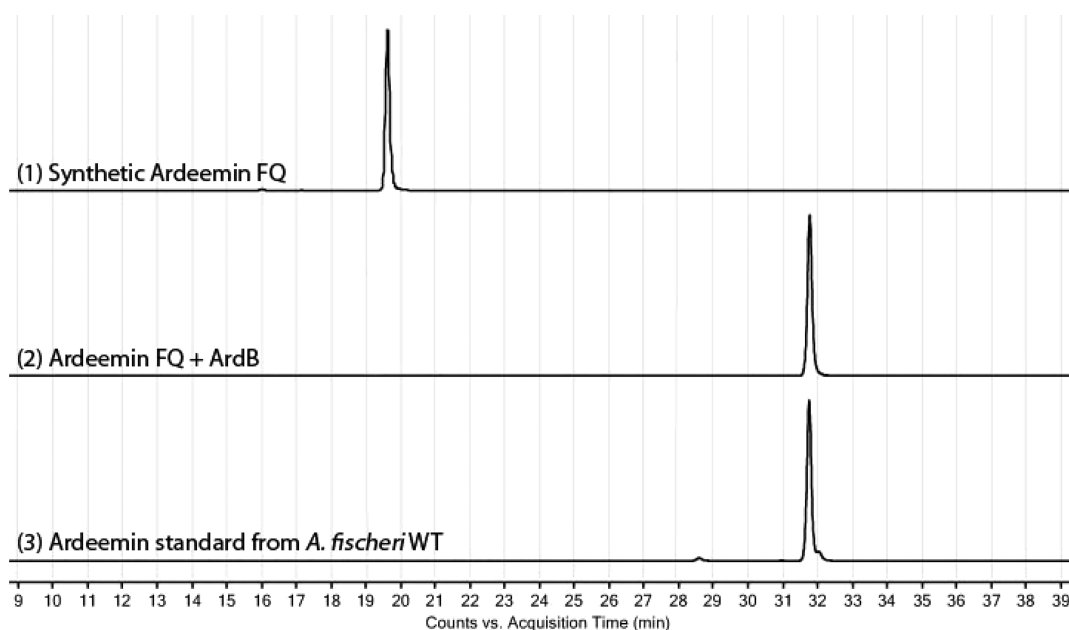


Figure 5. HR-LC-MS characterization of the transformation of synthetic ardeemin FQ to ardeemin by the action of ArdB and comparison to authentic ardeemin from *A. fischeri*. (1) EIC at m/z 359.1503. (2) EIC at m/z 427.2129. (3) EIC at m/z 427.2129.

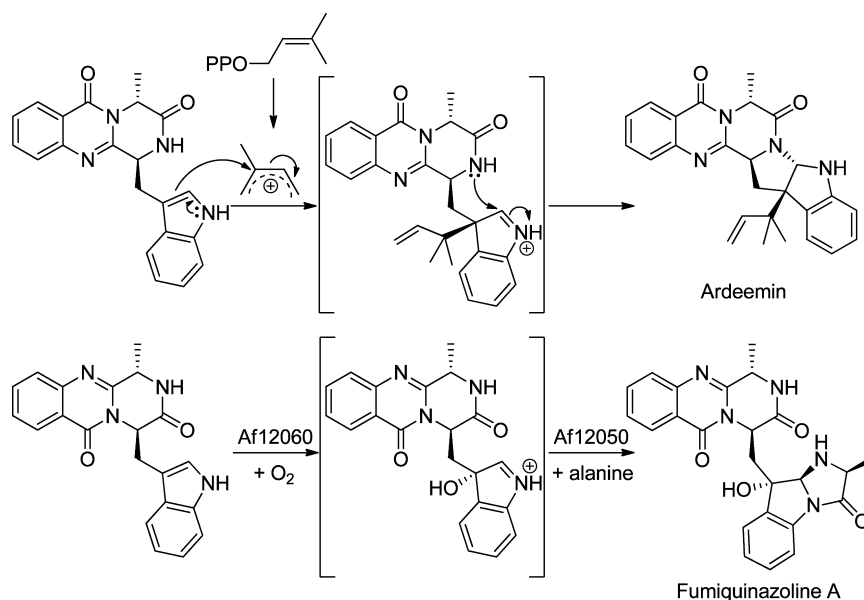
that draws ardeemin FQ forward to ardeemin. These knockout results support a simple two-enzyme pathway, ArdA followed by ArdB, to produce the hexacyclic scaffold of ardeemin from the three amino acids Ant, D-Ala, and L-Trp.

Heterologous Expression of the ArdA Protein in Yeast: *in Vivo* and *in Vitro* Findings. The *ardA* gene, encoding the three module 432 kDa ArdA protein was cloned in five pieces and assembled using a modified yeast *in vivo* recombination method as previous described, with removal of the one detected intron, to yield an N-terminal FLAG-tagged protein for expression in the vacuole protease-deficient *Saccharomyces cerevisiae* strain BJS464-NpgA that we have previously used for cloning the comparably sized trimodular TqaA¹⁴ (Figure 4b). Yeast cells expressing ArdA indeed generated the tricyclic ardeemin FQ metabolite as judged by LC-MS analysis (Figure 4a, trace 3). This is confirmed to be ardeemin FQ by mass analysis and its coelution with synthetic

ardeemin FQ (the regioisomeric FQF has a distinct retention time, data not shown).

Purification of the tagged ArdA from the yeast cells yields a soluble high molecular weight (~430 kDa) protein at ~1 mg/L (Figure 4b) that is sufficient to convert Ant, L-Ala, and L-Trp into ardeemin FQ, clearly distinct from the fumiquinazoline F (FQF) isomer (Figure 4a, trace 2). Rate data for purified ArdA indicate linear production over a 3-h incubation period at a turnover number of 17 ± 0.96 h⁻¹ (Figure 4c) under the assay conditions detailed in the Supporting Information. This is comparable to the turnover number of 23 h⁻¹ for TqaA as it produces the regioisomeric FQF.¹⁴ We had the four possible ardeemin FQ diastereomers available from our synthesis and therefore could confirm that ArdA results in isomerization of the added L-Ala into a D-Ala residue, most likely by the E(pimerase) domain of module two during tripeptide chain elongation (Scheme 1).

Scheme 2. Comparison of Post-NRPS Tailoring of FQ Scaffolds in Fumiquinazoline and Ardeemin Pathways: Capture of C- β of a Trp-Derived Indole Moiety by Oxygen (Fumiquinazoline) versus Carbon (Ardeemin) Electrophiles



Intriguingly, the trimodular NRPS ArdA has the same domain organization as TqaA and Af12050 from the tryptoqualanine⁵ and fumiquinazoline clusters,¹³ respectively. In those two NRPS trimodular cases genetics and biochemistry have validated the activation of anthranilate, L-Trp, and L-Ala, where the specificity of the three modules in TqaA and Af12080 is Ant₁-L-Trp₂-L-Ala₃, and the resulting product is the tricyclic fumiquinazoline F.^{5,13,14} In contrast, for ArdA it must be Ant₁-L-Ala₂-L-Trp₃, seemingly resulting from a functional swap in the order/specificity of module 2 and module 3. Unfortunately, examination of the amino acid recognition “code” of A domains from module 2 and 3 of TqaA and ArdB reveals little insight in to any shared genetic heritage of these domains or a clear indication of how this functional swap may have come about (Supplementary Table S3). Notably, all three of these trimodular NRPSs have four domains in module 2 (C₂-A₂T₂-E), where E is an epimerization domain. In agreement with the placement of that epimerization domain both residues activated by module 2 undergo epimerization, resulting in the incorporation of D-Trp₂ in FQF and D-Ala₂ in ardeemin FQ. All three NRPS enzymes end with a terminal C_T domain in module 3. We have shown for TqaA that this terminal C_T domain is required for cyclization/release of the tethered tripeptidyl-S-NRPS intermediate.¹⁴ For ArdA that intermediate would be the linear tripeptidyl thioester, covalently tethered as Ant₁-L-Ala₂-L-Trp₃-S-T domain (T₃). Scheme 1 shows the two distinct tethered tripeptidyl thioesters and compares their cyclization to the regioisomers FQF and ardeemin FQ by their respective trimodular NRPS enzymes, TqaA and ArdA. We propose that cyclization to give ardeemin FQ and FQF is mediated by an analogous series of events. First, attack by the free amine of Ant₁ on the thioester carbonyl of the corresponding (isomeric) linear tripeptide yields a 6,10 bicyclic nascent product. These bicyclic intermediates then undergo a transannular cyclodehydration to generate the tricyclic quinazolinone framework characteristic of FQF and ardeemin FQ (Supplementary Figure S6).

Heterologous Expression and Assay of ArdB as an Ardeemin FQ Prenyltransferase. To further complement

the genetic studies with biochemical ones, we next turned to assay of purified ArdB since we had synthesized its putative substrate ardeemin FQ as noted above. The *ardB* gene was cloned from *A. fischeri* cDNA (further details discussed in Supporting Information) and expressed in *Escherichia coli* as a soluble N-terminally tagged His₆-protein to allow affinity purification (Supplementary Figure S7).

Purified ArdB was then assayed with the separated diastereomers of synthetic ardeemin FQ in the presence of cosubstrate dimethylallyl diphosphate (further details discussed in Supporting Information). As shown in Figure 5 ardeemin FQ was converted to a product with the mass of mature ardeemin and had a retention time identical to that of authentic ardeemin isolated from the parent *A. fischeri* cultures. NMR analysis of the product from a preparative scale incubation confirmed the product was indeed ardeemin (Supplementary Figures S8 and S9). The regioisomeric FQF and *dia*-ardeemin FQ were both poor substrates for ArdB and produced minor mixtures of distinct products that were beyond the scope of these investigations, other than to note that ArdB is sensitive to the scaffolding context in which the indole ring is presented.

The substrate differentiation by ArdB between FQF (and *dia*-ardeemin FQ) and ardeemin FQ illustrates how the distinct substitution pattern (and even stereochemistry) of the released tricyclic-6,6,6- pyrazinoquinazolinones (FQF vs Ardeemin FQ) directs outcomes to dramatically different mature scaffolds by the action of subsequent tailoring enzymes (Scheme 2). The FQF scaffold gets processed at C₂ and C₃ of the indole side chain via oxygen insertion and alanine annulation by the tandem action of a flavoprotein and a monomodular NRPS pair to make FQA.¹⁵ The flavoenzyme (Af12060) acts on the indole 2,3-double bond to generate a transient hydroxyiminium species (via FAD-4a-OOH as electrophilic oxygen donor) that is then captured by the amine of the incoming alanyl-S-monomodular NRPS (Af12050) (Scheme 2, line 2). In contrast, the ardeemin FQ undergoes an analogous capture at C₂ of the indole moiety of the tryptophan side chain by an electrophile. However, the electrophile is not a flavin hydroperoxide but rather the delocalized carbocation resulting

from the cleavage of dimethylallyl diphosphate by an S_N1 type C-OPP cleavage in the active site of ArdB (Scheme 2, line 1). The resulting allylic C_1 cation is delocalized with charge deficiency also at C_3 and the carbon-carbon bond that forms is between the indole C_2 and the C_3 of the allyl cation to give a "reverse prenylation regiochemistry". The prenylated iminium ion (equivalent to the hydroxyiminium ion in the fumiquinazolinone system) can then be captured intramolecularly by the amide nitrogen of the pyrazinone ring, which was originally the amine nitrogen of Trp₃. The amide NH is a weak nucleophile but its intramolecular location generates a high local concentration. This creates a new N-C bond, joins the indole side chain to the pyrazinoquinazolinone system, and generates a fused hexacyclic 6-6-6-5-5-6 ring scaffold.

Conclusion. We can see that nature generates two dramatically different architecturally complex products, ardeemin and FQA, from related isomeric precursors using comparable enzymatic logic, activation by incoming electrophile (flavin hydroperoxide or allylic cation) setting up for a subsequent nucleophilic attack on C_2 of the indole substituent. The indole ring prenylation strategy that sets up the electrophilic species captured intramolecularly by an amide nitrogen during the biosynthesis of ardeemin is also exemplified in several other peptide contexts. These include the formation of the tricyclic pyrroloindole moiety in the cyclic hexadepsipeptide kutzneride antifungal agents^{24,25} and also in Bacillus competence factor peptides.²⁶⁻²⁹ In the case of ardeemin the amide nitrogen responsible for the intramolecular capture of the prenylated indole is part of a tricyclic moiety so the three ring (pyrazinoquinazolinone) unit joins the two ring indole unit by forming a bridging five ring. The net result is dramatic scaffold complexity and architectural constraint generation, all from the action of only two enzymes. Comparable logic in the fungal pathway to azonalenin also employs only two enzymes, the first a bimodular (rather than trimodular) NRPS, using anthranilate and Trp, to yield the 6,7-benzodiapinedione.¹² The second prenylating enzyme therefore generates a 6-7-5-5-6 pentacyclic array in that case rather than a hexacyclic framework.

The construction of scaffold complexity in the ardeemin peptidyl alkaloid is remarkably efficient. Only two enzymes are in play to convert three amino acid building blocks into the highly constrained fused hexacyclic product architecture. The first enzyme uses anthranilate as a starter and that planar β -amino acid creates architecture prone to cyclization that gives the 6-6-6 ardeemin FQ-type scaffold. Nature has performed a functional swap between the FQ and ardeemin FQ trimodular NRPS assemblies, switching Ala and Trp between positions two and three to give regioisomeric tricyclic pyrazinoquinazolinone products, FQ and ardeemin FQ, that are then vectored down distinct maturation pathways. These NRPS assembly lines are remarkable pathway-initiating catalysts. When paired with either indole oxygenase and/or indole prenyltransferase tailoring enzymes, they form branch points to distinct complex peptidyl indole alkaloid molecular frameworks in short two enzyme pathways. These anthranilate-derived tripeptides have been morphed into a range of multicyclic architectures that populate interesting chemical and biological space.⁴ Mixing and matching distinct anthranilate-initiating NRPS assembly lines with tailoring enzymes that perform electrophilic chemistry on a partner tryptophan side chain may allow engineering of new biologically active architecturally constrained scaffolds.

METHODS

Growth of *A. fischeri* (WT and Mutants) and Analysis of Metabolite Production. *A. fischeri* cultures were grown in liquid culture in both shake flasks and stationary cultures using glucose minimal media (GMM) (see Supplementary Tables S5-S7). Shake flask cultures were prepared by inoculating 50 mL of GMM in 250 mL baffled flasks with *A. fischeri* spore stock (see Supporting Information), and the resulting cultures were grown at 37 °C for 5 days. Stationary cultures were prepared by inoculating 10 mL of GMM in 60 × 15 mm Petri dishes, and the resulting cultures were grown at 28 °C for 4-5 days. Media from cultures was then extracted with an equal portion of ethyl acetate. Ethyl acetate was concentrated *in vacuo* to dryness, and the residue was resuspended in 50% acetonitrile/water and filtered for analysis by LC-MS.

Fungal Transformation and Gene Disruption in *A. fischeri*. Poly(ethylene glycol)-mediated transformation of *A. fischeri* was performed essentially as described previously.^{2,3} The homologous regions flanking the resistant marker were increased to ~2 kb, and other steps for construction of fusion PCR knockout cassettes containing the *bar* gene were performed as described elsewhere.³⁰ Glufosinate (~8 mg mL⁻¹) used for the selection of *bar* transformants was prepared as described previously.³¹ Approximately ~50 glufosinate-resistant transformants were picked and screened with PCR using a *bar* gene primer and primers outside of the deletion cassette as previously described (Supplementary Figure S3 and Table S8).³¹

Bioinformatic Analysis of *A. fischeri* Draft Genome and Identification of *ard* Cluster. Genomic DNA isolated from *A. fischeri* (see Supporting Information) was sequenced using Illumina shotgun sequencing. A total of 203,307,262 reads were assembled into 891 contigs. Contigs were used to generate a BLAST search database using standalone blast program (Blast C++). tBlastn (translated nucleotide database search using protein query) using Af12080 module 1 A-domain (anthranilate activating A-domain) identified two strong candidates for Ant-activating NRPS. Contigs containing candidate clusters were examined using eukaryotic gene predictor FGENESH (Softberry), and predicted proteins surrounding the candidate Ant-activating NRPS were examined by repeated BLAST search. Of those identified only one was found nearby an associated prenyltransferase and was therefore designated as the candidate *ard* cluster.

Synthesis of Ardeemin FQ and DMAPP Cofactor. Ardeemin FQ was synthesized by microwave accelerated condensation by analogy with the published procedure for the synthesis of FQF (see Supporting Information). Diastereomers and enantiomers were separated by HPLC over reverse phase and homochiral stationary phase columns (see Supporting Information). DMAPP was synthesized by analogy with the published procedure for the synthesis of geranyl diphosphate.³²

Cloning of ArdA. Cloning of the intact *ardA* gene into the expression vector was performed using the modified yeast-based homologous recombination method as described previously.^{14,33} The gene encoding ArdA was divided into four pieces (P1-P4) with a maximum size of ~4 kb. The only intron (475-547 base pairs (bp)) of the ArdA-encoding gene within P1 was removed by PCR with reverse transcription (RT-PCR). P2 to P4 were PCR amplified from the genomic DNA of *A. fischeri*. Each successive piece was designed to overlap (35-40 bp) with the two flanking ones, and the 5' end of P1 and 3' end of P4 overlap with the expression vector. The vector fragment was generated by digesting pXW55 (an expression vector with an engineered Flag tag on its N terminus and a His₆ tag on its C terminus) with SpeI and PmlI.³⁴ The individual pieces (1 μ g per piece) and the vector (~0.5 μ g) were transformed together using the EasyComp Transformation Kit (Invitrogen) into *S. cerevisiae* strain BJ5464-NpgA to allow assembly of the entire gene *in vivo*. The assembled plasmid was miniprep from *S. cerevisiae* using a yeast plasmid miniprep II kit (Zymo) and was further verified by PCR and restriction enzyme digestion.

Cloning of ArdB. *A. fischeri* total RNA isolated using a Qiagen RNeasy Plant Mini Kit using buffer RLC for cell lysis and performing

on-column DNase digestion. Oligo(dT)20 primers were used with SuperScript III First Strand Synthesis System (Invitrogen) for RT-PCR to generate *A. fischeri* cDNA. ArdB was cloned into pET30 Ek/LIC using the corresponding vector kit (EMD) N-terminal His₆-S-tagged. PCR reactions were primed with 5'-GACGACGACAAGAT-GACATTACATCTTCCGCC-3' and 5'-GAGGA-GAAGCCCGTCAACCAGTGGTAATATATGGACAGGTAGG-GAC-3' (where underlined sequence denotes sequence complementary to the gene).

Protein Expression and Purification. The verified plasmid containing the intact ArdB-encoding genes was transformed into *S. cerevisiae* strain BJ5464-NpgA for protein expression. For 1 L of yeast culture, the cells were grown at 28 °C in yeast extract peptone dextrose medium with 1% (w/v) dextrose for 72 h. The cells were harvested by centrifugation (2500 g, 20 min, 4 °C), resuspended in 20 mL lysis buffer (50 mM NaH₂PO₄ pH 8.0, 0.15 M NaCl, 10 mM imidazole) and lysed using sonication on ice. Lysate was centrifuged at 35,000 g for 60 min at 4 °C to remove cellular debris. FLAG-tagged proteins were purified by using ANTI-FLAG M1 Agarose Affinity Gel (Sigma-Aldrich), following the supplied protocols. The cleared cell lysate was applied onto a gravity flow column with packed ANTI-FLAG Agarose Affinity Gel. After washing steps as standard protocols, the protein was eluted with the FLAG peptide elution buffer (0.5 mg mL⁻¹ FLAG peptide, 50 mM Tris-HCl, pH 7.4, 100 mM NaCl).

ArdB was overproduced in *E. coli* BL21 (DE3) cells (Stratagene). Four liters of cells were grown at 37 °C in LB (plus 50 µg/mL kanamycin) to an OD₆₀₀ between 0.4 and 0.8, and the temperature was lowered to 16 °C prior to induction with 0.2 mM IPTG. Cells were harvested 18–24 h postinduction by centrifugation, suspended in lysis buffer (25 mM Tris-HCl [pH 7.5], 300 mM NaCl, 20% glycerol, 0.1% Tween 20, and lysed using a EmulsiFlex-C5 homogenizer (Avestin). Insoluble material was removed by centrifugation (35,000g) and soluble protein applied to 1–2 mL of Ni-NTA agarose (Qiagen). ArdB was purified to near homogeneity (Figure 4) by Ni-affinity purification; protein was batch bound to Ni-resin for 30 min at 4 °C, Ni-resin was washed with 2 × 25 mL buffer A (50 mM Tris-HCl [pH 7.5], 300 mM NaCl, 10% glycerol, 0.1 mM EDTA) containing 20 mM imidazole, and protein was eluted with buffer A containing 250 mM imidazole (2 × 5 mL). Elutions containing ArdB (>90% pure, see Supporting Information) were pooled and concentrated using centrifugal filtration devices (Amicon, 30,000 MWCO) and then flash-frozen in liquid N₂ and stored at –80 °C.

In Vitro Assay of ArdB. To test the *in vitro* activities of ArdB, 2 mM of each amino acid building block, 6 mM ATP, 4 mM MgSO₄ and 10 µM of purified ArdB in 50 mM Tris-HCl buffer (pH 7.5) to a total volume of 100 µL. After a 12-h incubation, the reaction was quenched and extracted with 1 mL of ethyl acetate. The organic layer was dried, redissolved in methanol, and injected onto a Shimadzu 2010 EV LC mass spectrometer using positive and negative electrospray ionization and a Phenomenex Luna 5 µm, 2.0 mm × 100 mm C18 reverse-phase column. Samples were separated on a linear gradient of 5–95% (v/v) CH₃CN in water (0.1% (v/v) formic acid) for 30 min at a flow rate of 0.1 mL min⁻¹ followed by isocratic 95% (v/v) CN in water (0.1% (v/v) formic acid) for 15 min. Under these conditions Ardeemin FQ was eluted at 23.5 min.

HPLC-Based Time Course Study of Product Formation by ArdB. Reactions (500 µL) contained 1 µM ArdB, 3 mM ATP, 2 mM MgCl₂, and 1 mM amino acid substrates (Ant, L-Trp, and L-Ala) in 50 mM Tris-HCl buffer (pH 7.5). Reactions were incubated at 25 °C, and 100 µL aliquots were taken at 1, 2, 3, and 4 h after addition of enzyme and extracted with 1 mL of ethyl acetate. Only data points within the linear range were used to calculate the initial product formation rates. The fitted slope of the linear portion of initial turnover is 17.36 h⁻¹, with R² = 0.992. Data represent mean values ± SD. The organic layer was dried and redissolved in 100 µL of methanol, and 20 µL samples were injected for LC–MS analyses. Integration of the Ardeemin FQ peak (at 292 nm) was used to generate a plot of product peak area vs time in order to approximate enzymatic rate. Initial rate data (obtained as integration area per hour) was converted to µM per hour using

standard curves generated from 20 µL injections of Ardeemin FQ sample of known concentration.

HPLC-Based Assays for ArdB Activity. Reaction mixtures were set up containing 5 µM ArdB, 2 mM DMAPP (see Supporting Information), 5 mM calcium chloride, and 100 µM ardeemin FQ in Tris-HCl buffer [50 mM sodium phosphate (pH 7.5), 100 mM NaCl and 5% glycerol]. Reactions were initiated by the addition of ArdB and were incubated at 37 °C overnight (14–16 h). Reactions were then quenched by the addition of an equal volume of acetonitrile, the precipitant was removed by centrifugation, and 20 µL samples of the resulting supernatant were injected for HPLC analysis on a Beckmann Coulter Gold system equipped with an Alltima C18 reverse-phase column (150 × 4.6 mm, 5 µm). Solvent system A (water plus 0.1% TFA) and B (acetonitrile plus 0.1% TFA) held at 25% B for 1 min and then run over a linear gradient of 25–55% B over 20 min, followed by a gradient of 55–95% B over 1 min before a holding at 95% B for 2.5 min, and the column was then equilibrated back to initial conditions by returning to 25% B and holding for 5 min. Reactions were scaled up to 15 mL to allow for isolation and characterization of their corresponding products (see Supporting Information).

■ ASSOCIATED CONTENT

● Supporting Information

Additional experimental procedures including the synthesis of ardeemin FQ, HPLC purification protocols, sequencing statistics, summary of bioinformatics analysis isolation of genomic DNA, protocol of genetic disruption, LC–HRMS comparisons and NMR spectroscopic data. This material is available free of charge via the Internet at <http://pubs.acs.org>.

■ AUTHOR INFORMATION

Corresponding Author

*E-mail: yitang@ucla.edu; christopher_walsh@hms.harvard.edu.

Notes

The authors declare no competing financial interest.

■ ACKNOWLEDGMENTS

We thank the National Institutes of Health for funding [GM20011, GM49338 (to C.T.W.) and GM092217 (to Y.T.)].

■ REFERENCES

- (1) Fremlin, L. J., Piggott, A. M., Lacey, E., and Capon, R. J. (2009) Cottoquinazoline A and cotteslosins A and B, metabolites from an Australian marine-derived strain of *Aspergillus versicolor*. *J. Nat. Prod.* 72, 666–670.
- (2) Jiao, R. H., Xu, S., Liu, J. Y., Ge, H. M., Ding, H., Xu, C., Zhu, H. L., and Tan, R. X. (2006) Chaetominine, a cytotoxic alkaloid produced by endophytic *Chaetomium* sp. *IFB-E015. Org. Lett.* 8, 5709–5712.
- (3) Wong, S. M., Musza, L. L., Kydd, G. C., Kullnig, R., Gillum, A. M., and Cooper, R. (1993) Fiscalins: new substance P inhibitors produced by the fungus *Neosartorya fischeri*. Taxonomy, fermentation, structures, and biological properties. *J. Antibiot. (Tokyo)* 46, 545–553.
- (4) Walsh, C. T., Haynes, S. W., and Ames, B. D. (2012) Aminobenzoates as building blocks for natural product assembly lines. *Nat. Prod. Rep.* 29, 37–59.
- (5) Gao, X., Chooi, Y. H., Ames, B. D., Wang, P., Walsh, C. T., and Tang, Y. (2011) Fungal indole alkaloid biosynthesis: Genetic and biochemical investigation of the tryptoguanine pathway in *Penicillium aethiopicum*. *J. Am. Chem. Soc.* 133, 2729–2741.
- (6) Takahashi, C., Matsushita, T., Doi, M., Minoura, K., Shingu, T., Kumeda, Y., and Numata, A. (1995) Fumiquinazolines A-G, novel metabolites of a fungus separated from a *Pseudolabrus* marine fish. *J. Chem. Soc., Perkin Trans. 1*, 2345–2353.
- (7) Chang, R., Lotti, V., Monaghan, R., Birnbaum, J., Stapley, E., Goetz, M., Albers-Schonberg, G., Patchett, A., Liesch, J., Hensens, O.,

- et al. (1985) A potent nonpeptide cholecystokinin antagonist selective for peripheral tissues isolated from *Aspergillus alliaceus*. *Science* 230, 177–179.
- (8) Liesch, J. M., Hensens, O. D., Zink, D. L., and Goetz, M. A. (1988) Novel cholecystokinin antagonists from *Aspergillus alliaceus*. II. Structure determination of asperlicins B, C, D, and E. *J. Antibiot. (Tokyo)* 41, 878–881.
- (9) Karwowski, J. P., Jackson, M., Rasmussen, R. R., Humphrey, P. E., Poddig, J. B., Kohl, W. L., Scherr, M. H., Kadam, S., and McAlpine, J. B. (1993) 5-N-acetylardeemin, a novel heterocyclic compound which reverses multiple drug resistance in tumor cells. I. Taxonomy and fermentation of the producing organism and biological activity. *J. Antibiot. (Tokyo)* 46, 374–379.
- (10) Hochlowski, J. E., Mullally, M. M., Spanton, S. G., Whittern, D. N., Hill, P., and McAlpine, J. B. (1993) 5-N-Acetylardeemin, a novel heterocyclic compound which reverses multiple drug resistance in tumor cells. II. Isolation and elucidation of the structure of 5-N-acetylardeemin and two congeners. *J. Antibiot. (Tokyo)* 46, 380–386.
- (11) Finking, R., and Marahiel, M. A. (2004) Biosynthesis of nonribosomal peptides. *Annu. Rev. Microbiol.* 58, 453–488.
- (12) Yin, W. B., Grundmann, A., Cheng, J., and Li, S. M. (2009) Acetylazonalenin biosynthesis in *Neosartorya fischeri*. Identification of the biosynthetic gene cluster by genomic mining and functional proof of the genes by biochemical investigation. *J. Biol. Chem.* 284, 100–109.
- (13) Ames, B. D., and Walsh, C. T. (2010) Anthranilate-activating modules from fungal nonribosomal peptide assembly lines. *Biochemistry* 49, 3351–3365.
- (14) Gao, X., Haynes, S. W., Ames, B. D., Wang, P., Vien, L. P., Walsh, C. T., and Tang, Y. (2012) Cyclization of fungal nonribosomal peptides by a terminal condensation-like domain. *Nat. Chem. Biol.* 8, 823–830.
- (15) Ames, B. D., Liu, X., and Walsh, C. T. (2010) Enzymatic processing of fumiquinazoline F: a tandem oxidative-acylation strategy for the generation of multicyclic scaffolds in fungal indole alkaloid biosynthesis. *Biochemistry* 49, 8564–8576.
- (16) Ames, B. D., Haynes, S. W., Gao, X., Evans, B. S., Kelleher, N. L., Tang, Y., and Walsh, C. T. (2011) Complexity generation in fungal peptidyl alkaloid biosynthesis: Oxidation of fumiquinazoline A to the heptacyclic hemiaminal fumiquinazoline C by the flavoenzyme Af12070 from *Aspergillus fumigatus*. *Biochemistry* 50, 8756–8769.
- (17) Juliano, R. L., and Ling, V. (1976) A surface glycoprotein modulating drug permeability in Chinese hamster ovary cell mutants. *Biochim. Biophys. Acta* 455, 152–162.
- (18) Kartner, N., Riordan, J. R., and Ling, V. (1983) Cell surface P-glycoprotein associated with multidrug resistance in mammalian cell lines. *Science* 221, 1285–1288.
- (19) Chou, T. C., Depew, K. M., Zheng, Y. H., Safer, M. L., Chan, D., Helfrich, B., Zatorska, D., Zatorski, A., Bornmann, W., and Danishefsky, S. J. (1998) Reversal of anticancer multidrug resistance by the ardeemins. *Proc. Natl. Acad. Sci. U.S.A.* 95, 8369–8374.
- (20) Depew, K. M., Marsden, S. P., Zatorska, D., Zatorski, A., Bornmann, W. G., and Danishefsky, S. J. (1999) Total synthesis of 5-N-acetylardeemin and amauromine: Practical routes to potential MDR reversal agents. *J. Am. Chem. Soc.* 121, 11953–11963.
- (21) Liu, J.-F., Ye, P., Zhang, B., Bi, G., Sargent, K., Yu, L., Yohannes, D., and Baldino, C. M. (2005) Three-component one-pot total syntheses of gyantrypine, fumiquinazoline F, and fiscalin B promoted by microwave irradiation. *J. Org. Chem.* 70, 6339–6345.
- (22) Haynes, S. W., Ames, B. D., Gao, X., Tang, Y., and Walsh, C. T. (2011) Unraveling terminal C-domain-mediated condensation in fungal biosynthesis of imidazoindolone metabolites. *Biochemistry* 50, 5668–5679.
- (23) Avalos, J., Geever, R. F., and Case, M. E. (1989) Bialaphos resistance as a dominant selectable marker in *Neurospora crassa*. *Curr. Genet.* 16, 369–372.
- (24) Broberg, A., Menkis, A., and Vasiliauskas, R. (2006) Kutznerides 1–4, depsipeptides from the actinomycete *Kutzneria* sp. 744 inhabiting mycorrhizal roots of *Picea abies* seedlings. *J. Nat. Prod.* 69, 97–102.
- (25) Fujimori, D. G., Hrvatin, S., Neumann, C. S., Strieker, M., Marahiel, M. A., and Walsh, C. T. (2007) Cloning and characterization of the biosynthetic gene cluster for kutznerides. *Proc. Natl. Acad. Sci. U.S.A.* 104, 16498–16503.
- (26) Akrigg, A., Ayad, S. R., and Barker, G. R. (1967) The nature of a competence-inducing factor in *Bacillus subtilis*. *Biochem. Biophys. Res. Commun.* 28, 1062–1067.
- (27) Magnuson, R., Solomon, J., and Grossman, A. D. (1994) Biochemical and genetic characterization of a competence pheromone from *B. subtilis*. *Cell* 77, 207–216.
- (28) Okada, M., Sato, I., Cho, S. J., Iwata, H., Nishio, T., Dubnau, D., and Sakagami, Y. (2005) Structure of the *Bacillus subtilis* quorum-sensing peptide pheromone ComX. *Nat. Chem. Biol.* 1, 23–24.
- (29) Okada, M., Yamaguchi, H., Sato, I., Tsuji, F., Dubnau, D., and Sakagami, Y. (2008) Chemical structure of posttranslational modification with a farnesyl group on tryptophan. *Biosci. Biotechnol. Biochem.* 72, 914–918.
- (30) Szweczyk, E., Nayak, T., Oakley, C. E., Edgerton, H., Xiong, Y., Taheri-Talesh, N., Osmani, S. A., and Oakley, B. R. (2006) Fusion PCR and gene targeting in *Aspergillus nidulans*. *Nat. Protoc.* 1, 3111–3120.
- (31) Gao, X., Chooi, Y. H., Ames, B. D., Wang, P., Walsh, C. T., and Tang, Y. (2011) Fungal indole alkaloid biosynthesis: Genetic and biochemical investigation of the tryptoquialanine pathway in *Penicillium aethiopicum*. *J. Am. Chem. Soc.* 133, 2729–2741.
- (32) Woodside, A. B., Huang, Z., and Poulter, C. D. (1988) Trisammonium gerynol diphosphate. *Org. Synth.* 66, 211–219.
- (33) Shao, Z., Zhao, H., and Zhao, H. (2009) DNA assembler, an in vivo genetic method for rapid construction of biochemical pathways. *Nucleic Acids Res.* 37, No. e16.
- (34) Xu, W., Cai, X. L., Jung, M. E., and Tang, Y. (2010) Analysis of intact and dissected fungal polyketide synthase-nonribosomal peptide synthetase in vitro and in *Saccharomyces cerevisiae*. *J. Am. Chem. Soc.* 132, 13604–13607.

NOTE ADDED AFTER ASAP PUBLICATION

Reference 34 was a duplicate of Reference 14 in the version published ASAP February 6, 2013. The corrected version was re-posted on February 12, 2013.